Supporting Information

Direct observations of surface plasmon polaritons in highly conductive organic thin film

Jianhan Yang†, Hossam A. Almossalami†, Zhewei Wang†, Ke Wu†, Chen Wang‡, Kuan Sun‡, Yang (Michael) Yang,†, Hui Ye*,†*

†State Key Laboratory of Modern Optical Instrumentation, College of Optical Science and Engineering, Zhejiang University, Hangzhou, 310027, P. R. China

‡MOE Key Laboratory of Low-Grade Energy Utilization Technologies and Systems, School of Energy & Power Engineering, Chongqing University, Chongqing 400044, China

*Corresponding Author: Hui Ye, huiye@zju.edu.cn.; Yang (Michael) Yang, yangyang15@zju.edu.cn.

Section A The Supplement to Drude-Lorentz Dispersion Model

Considering the epsilon-near-zero wavelength region, the screened plasma frequency ω^{*} [1] is expressed by **Equation S1**:

$$\omega^{*} = \omega(\varepsilon' = 0) = \sqrt{\frac{{\omega_p}^2}{\varepsilon_\infty} - {\Gamma_D}^2} \tag{1}$$

which is also depends on the screening field produced by the valence electrons and related to the permittivities cross-over wavelength λ_C mentioned above. Meanwhile, the surface plasmon frequency[1] which represents the upper limit of the frequency to activate surface plasmon polaritons propagation mode can be written as **Equation S2**:

$$\omega_{sp} = \omega(\varepsilon' = -1) = \sqrt{\frac{{\omega_p}^2}{\varepsilon_\infty + 1} - {\Gamma_D}^2} \tag{2}$$

it is corresponding to the surface plasmon wavelength λ_{sp}.

Section B The Supplement to Propagation And Confinement of Surface Plasmon Polaritons

The real part of surface plasmon polaritons wave vector $\boldsymbol{{k_{spp}}'(\omega)}$.

When the incident p-polarized light enters the dielectric-metal interface shown in **Figure S1**, taking $k_0 = \frac{\omega_0}{c}$, from the Maxwell equation and Helmholtz equation, we can get:

$$\frac{\partial^2 \vec{E}(z)}{\partial z^2} + \left({k_0}^2 \varepsilon - \beta^2\right)\vec{E}(z) = 0 \tag{3}$$

where, $\beta = k_{spp}$, i.e. the wave vector in the x-direction.

For TM wave, solve this equation and for z<0, we can obtain that the:

$$E_x(z) = -iA_1 \frac{1}{\omega \varepsilon_0 \varepsilon_2} k_1 e^{i\beta x} e^{-k_1 z} \tag{4a}$$

$$E_z(z) = -A_1 \frac{\beta}{\omega \varepsilon_0 \varepsilon_2} k_1 e^{i\beta x} e^{-k_1 z} \tag{4b}$$

Where $k_1^2 = \beta^2 - k_0^2 \varepsilon$ (5)

Due to the continuity of the electromagnetic wave at the interface, we can get:

$$\beta = k_0 \sqrt{\frac{\varepsilon_1 \varepsilon_2}{\varepsilon_1 + \varepsilon_2}} \tag{6}$$

When surface plasmon polaritons occur, $\beta = k_{spp} = k_{\parallel}$. In the metal (z<0), $k_1 = ik_{\perp}$.

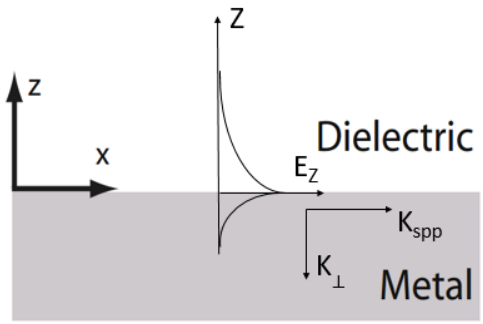

Figure S1.The schematic of surface plasmon polaritons

Assuming that the medium is air, the real part should be:

$$k_{spp}{}'(\omega) = Re(k_{\parallel}) = Re(k_{spp}) = Re\left(k_0\sqrt{\frac{\varepsilon_1}{\varepsilon_1+1}}\right) = Re(\frac{2\pi}{\lambda_0}\sqrt{\frac{\varepsilon(\omega)}{\varepsilon(\omega)+1}}) \quad (7)$$

ε(ω) is the permittivity of our modified PEDOT: PSS film. And then the dispersion curve of $k_{spp}{}'$ is plotted as follows:

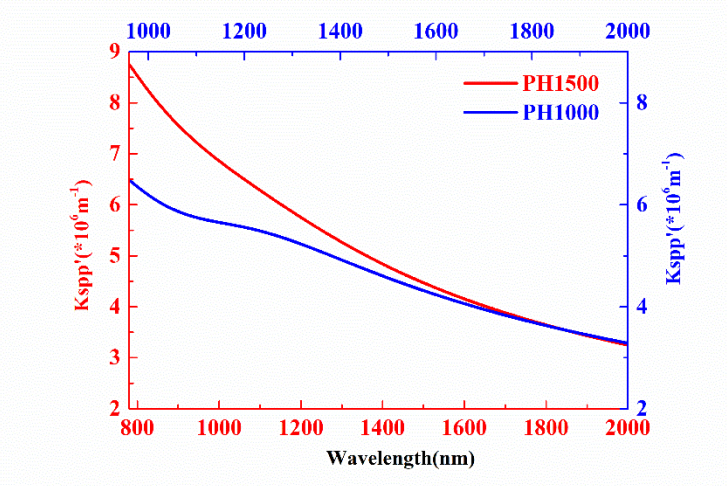

Figure S2. The wavelength-dependent surface plasmon polaritons wave vector $k_{spp}{}'$ of PH1500 (red line) and PH1000 (blue line).

It can be seen that $k_{spp}{}'(\omega)$ is actually decreasing with the increase of wavelength, which can explain why the resonant angle corresponding to reflectivity dip decreases when the incidence wavelength increase in prism coupling experiment.

The propagation length of surface plasmon polaritons $\delta_{spp}(\omega)$.

If the dielectric is air, in the metal, $k_{\perp} = ik_1$,

$$k_{\perp} = ik_1 = i\sqrt{\beta^2 - k_o{}^2\varepsilon(\omega)} = \frac{2\pi}{\lambda_0}\sqrt{\frac{\varepsilon(\omega)^2}{\varepsilon(\omega)+1}} \tag{8}$$

in the air, $k_{\perp \mathrm{d}} = ik_2$,

$$k_{\perp \mathrm{d}} = ik_2 = i\sqrt{\beta^2 - k_o{}^2\varepsilon_d} = \frac{2\pi}{\lambda_0}\sqrt{\frac{1}{\varepsilon(\omega)+1}} \tag{9}$$

and the expression of electric field vector function of the evanescent wave in metal:

$$\vec{E} = \vec{E}(z)e^{i\beta x} = \overrightarrow{E_0}e^{-k_1 z}e^{ik_{spp}x} \tag{10}$$

and k_{spp} can be divided into real and imaginary parts:

$$k_{spp} = k'_{spp} + \mathrm{i}k''_{spp} \tag{11}$$

substitute (11) into the above equation (10):

$$\vec{E} = \vec{E}(z)e^{ik'_{spp}x}e^{-k''_{spp}x} \tag{12}$$

among this, $e^{-k''_{spp}x}$ is the decay term, which determines the distance of the decay. When the electric field intensity after which the intensity decreases to 1/e, *i.e.* $k''_{spp}x = 1$, the propagation length is then given by :

$$\delta_{spp} = \frac{1}{K_{spp}{}''} = \frac{1}{Im(K_{\parallel})} = \frac{1}{Im(\beta)} = \frac{1}{Im(\frac{2\pi}{\lambda_0}\sqrt{\frac{\varepsilon(\omega)}{\varepsilon(\omega)+1}})} \tag{13}$$

The penetration depth of surface plasmon polaritons $\delta_{con}(\omega)$ and δ'_{con}.

Similarly, the penetration depth in the metal in the z-direction is defined as the intensity decays to 1/e of the original, i.e. $k''_{\perp}z = 1$, the penetration depth in the metal is then determined as:

$$\delta_{con} = \frac{1}{k_{\perp}''} = \frac{1}{Im(k_{\perp})} = \frac{1}{Im(\frac{2\pi}{\lambda_0}\sqrt{\frac{\varepsilon(\omega)^2}{\varepsilon(\omega)+1}})} \tag{14}$$

the penetration depth in the air is then determined as:

$$\delta'_{con} = \frac{1}{k_{\perp d}''} = \frac{1}{Im(k_{\perp d})} = \frac{1}{Im(\frac{2\pi}{\lambda_0}\sqrt{\frac{1}{\varepsilon(\omega)+1}})} \tag{15}$$

We draw the propagation lengths and skin penetration depths of ITO, Au and Ag to compared with those of PH1500 and PH1000 in **Figure S3**. And the permittivity of noble metals (Ag and Au) is obtained from ref. [2] and [3].

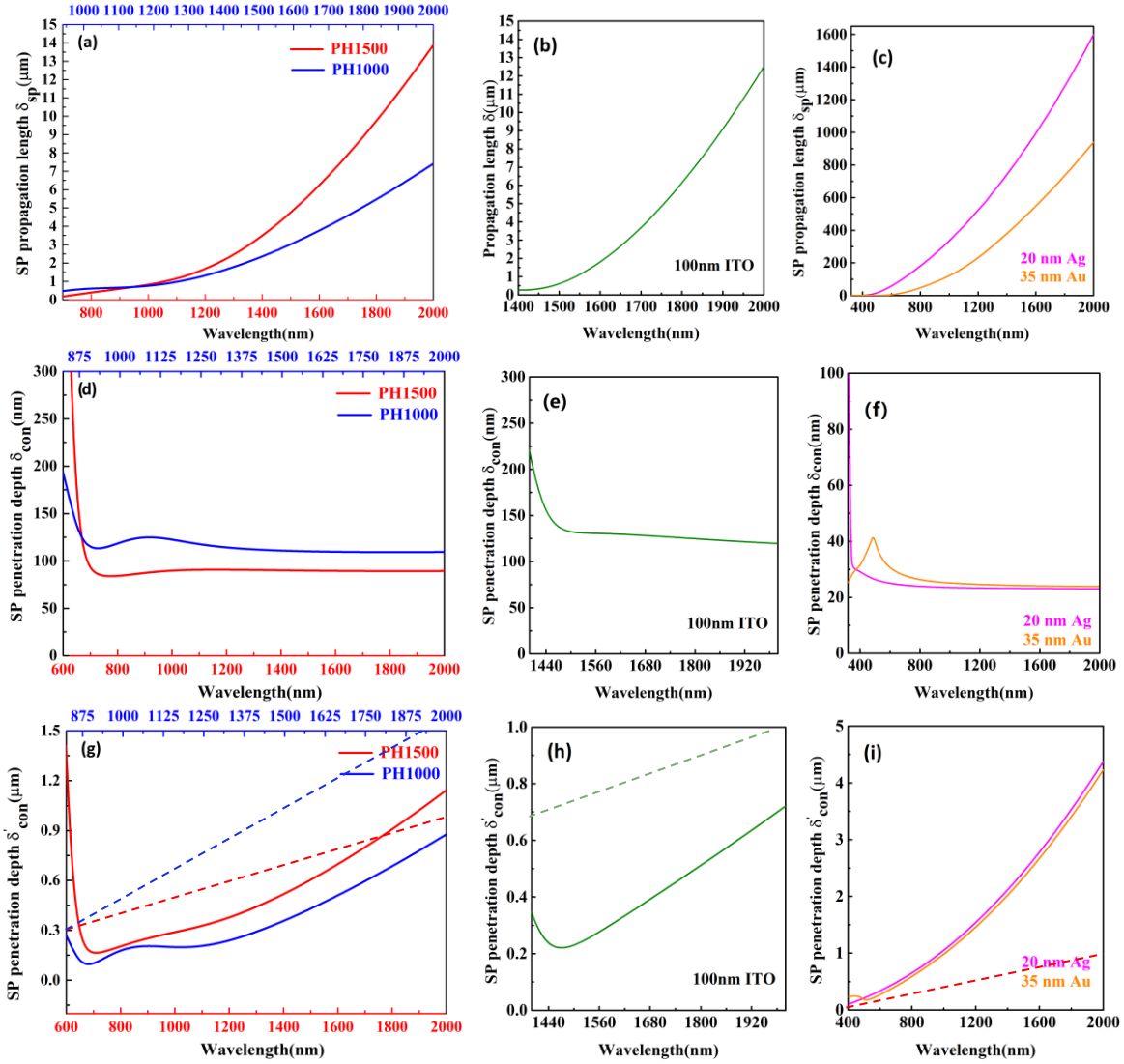

Figure S3. Surface plasmon polaritons profiles of modified PEDOT: PSS, ITO, Ag and Au thin films. (a) Surface plasmon propagation lengths δ_{spp} of PH1500 and PH1000. (b) δ_{spp} of ITO film for comparison. (c) δ_{spp} of Ag and Au. (d) Surface plasmon penetration depths in

the metal δ_{con} of PH1500 and PH1000. (e) δ_{con} of ITO film for analogy. (f) δ_{con} of Ag and Au. (g) Surface plasmon penetration depths in the air δ'_{con} of PH1500 and PH1000. (h) δ'_{con} of ITO film.(i) δ'_{con} of Ag and Au. The dash line in (g-i) corresponds to the upper compactness limit $\delta'_{con} = \lambda_0/2$.

It is visibly shown, surface plasmon polaritons of modified PEDOT: PSS films start to propagate from the wavelength around 800 nm, and can reach up to the utmost ~14 μm at 2000 nm. Longer propagation length can be realized by either lower imaginary part ε" or larger value of the real part |ε'|. PH1500 possesses both larger |ε'| and larger ε" in the wavelengths longer than λ_{sp} when compared with PH1000 (shown in Figure 2c, d). However, comprehensively considering the synthetic effect of both the real and imaginary permittivity, the fact that PH1500 owns a longer propagation length than PH1000 and ITO in the near infrared region is summarized in Figure S3a, b. While, the propagation lengths of PH1500, PH1000 and ITO are still two orders of magnitude smaller than the propagation lengths of Au and Ag, which can reach hundreds or even thousands of microns in the near infrared (Figure S3c). This derives from the slightly lower carrier concentrations of PH1500 and PH1000 which giving rise to the relative smaller magnitude of real part of the dielectric permitivities than noble metals. In Figure S3e, at low wavelengths, since surface plasmon polaritons is not excited in ITO film yet, only PEDOT: PSS films have constraint characteristics. And at the wavelengths longer than 1450 nm, the penetration depth of ITO is around 130 nm, which are a little larger than those of modified PEDOT: PSS in Figure S3d, but all of them are still larger than those of noble metals, which are less than 40 nm in 800-2000nm. This also indicates the relative superiority of noble metals in the confinement of surface plasmon polaritons in the thin film layer. In Figure S3g, h, i, one can see that the penetration depths δ'_{con} in the dielectric (air) of PH1500 and PH1000 films are 3 to 4 times smaller than those of Au and Ag, giving rise to better confinements in the dielectric side. Considering the

effective operating wavelength range of plasmonics, the PEDOT: PSS samples are qualified for a relative wider working wavelength region compared with ITO thin film in the near infrared range.

Section C Localized Surface Plasmon Resonance Simulation

In order to better clarify the plasmon performances of PH1500 and PH1000 thin films, we designed cylindrical micro-hole column array structures based on these films in the simulation software FDTD, as shown in **Figure S4**.

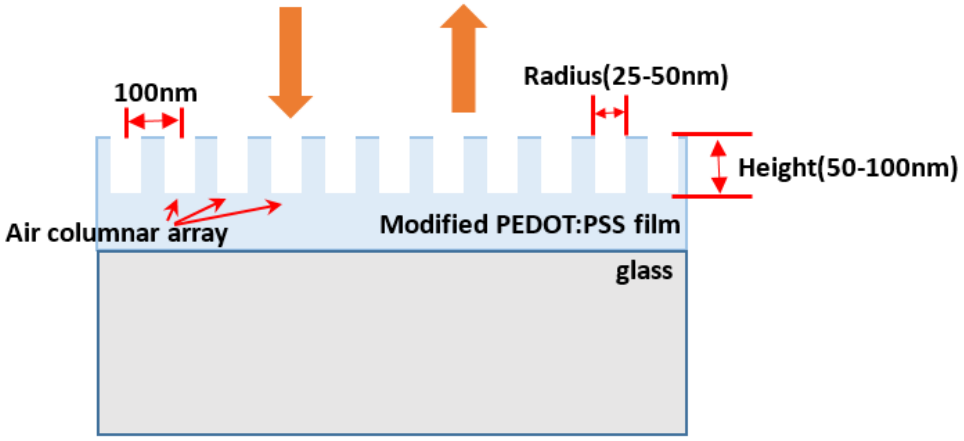

Figure S4. The side-view of air hole column array structures in the modified PEDOT: PSS films.

We changed the incident wavelength from 700 to 2000 nm to find out the best wavelength for localized surface plasmon resonance (LSPR) in each film. At the same time, by varying the structure radius from 25 nm to 50 nm, along with adjusting structure height, we can regulate the distribution and intensity of the field, and then obtain the maximum electric field enhancement. The simulation results of FDTD are as follows:

For PH1000, LSPR is obvious when the incident wavelength is at 1415 nm. As the height of air column is 90 nm and radius is 25 nm, it reaches a most uniform and intensive edge electric field enhancement with an intensity of above 1.9, as shown in **Figure S**5a. When the

radius of the structure reaches 28 nm and the height changes to 61 nm, an even more intense edge strengthening (around 2.3) can be achieved in Figure S5b. In addition to the case that the intensity is as high as above 5 in individual points, the enhancement in this condition is already the highest uniform value.

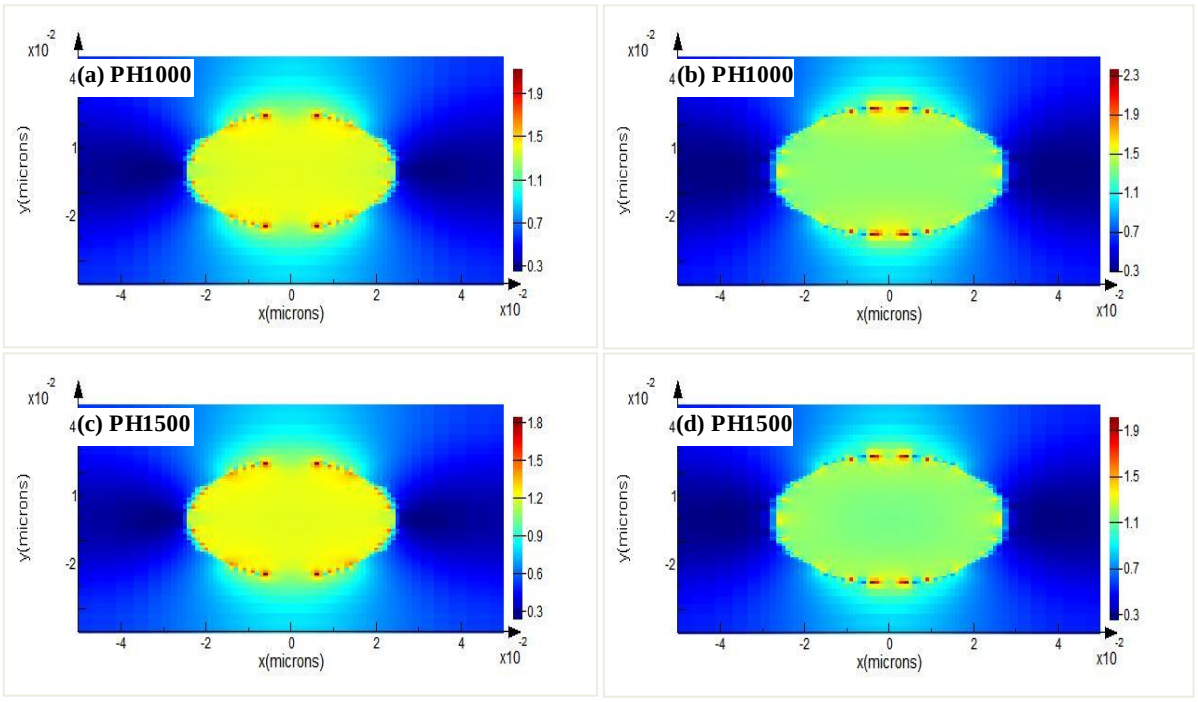

Figure S5. FDTD simulations of the near field distribution for cylindrical micro-hole column based on PH1000 and PH1500 thin films on glass substrates(top-view of single structure). (a) Near-field distribution of PH1000 (Air column height: 90 nm; radius: 25 nm). (b) Near-field distribution of PH1000 (Air column height: 61 nm; radius: 28 nm). (c) Near-field distribution of PH1500 (Air column height: 60 nm; radius: 25 nm). (d) Near-field distribution of PH1500 (Air column height: 50 nm; radius: 28 nm). The respective field enhancement is displayed according to the color scale valid for all panels. Directional light illumination is modeled in simulations at a central wavelength of 1415 nm for PH1000 and 1235 nm for PH1500. At this wavelength the plasmonic mode located at the cylindrical edge of structures is excited. And a maximum field enhancement factor of about 2.3 can be observed.

Similarly, for PH1500, the simulation is also carried out as shown in Figure S5c, d. LSPR is most obvious when the incident wavelength is 1235 nm this time. And Figure S5c is acquired from the air column array structure with a height of 60 nm and a radius of 25 nm, while the strongest enhancement happens at a height of 50 nm with a radius of 28 nm in Figure S5d. When we designed the structure, since the film thickness used for PH1500 simulation was set at 168 nm according to the real film thickness, which was less than 460 nm of PH1000, this leads to that the electric field enhancement result of PH1500 within the height range of our variation was slightly weaker than that of PH1000. However, this does not affect our identification on the LSPR of modified PEDOT: PSS films.

Supporting References

(1) Dominici, L.; Michelotti, F.; Brown, T. M.; Reale, A.; Di Carlo, A. Plasmon Polaritons in the Near Infrared on Fluorine Doped Tin Oxide Films. *Opt. Express* **2009,** *17*, 10155-10167.

(2) Ciesielski, A.; Skowronski, L.; Trzcinski, M.; Gorecka, E.; Trautman, P.; Szoplik, T. Evidence of Germanium Segregation in Gold Thin Films. *Surf. Sci.* **2018,** *674*, 73-78.

(3) Ciesielski, A.; Skowronski, L.; Trzcinski, M.; Szoplik, T. Controlling the Optical Parameters of Self-Assembled Silver Films with Wetting Layers and Annealing. *Appl. Surf. Sci.* **2017,** *421*, 349-356.